



Published in final edited form as:

*Histochem Cell Biol.* 2004 June ; 121(6): 493–499. doi:10.1007/s00418-004-0653-5.

## MEPE IS EXPRESSED DURING SKELETAL DEVELOPMENT AND REGENERATION

Chuangyong Lu, Steve Huang, Theodore Miclau, Jill A. Helms, and Céline Colnot \*

### Abstract

Matrix extracellular phosphoglycoprotein (MEPE) is a bone metabolism regulator that is expressed by osteocytes in normal adult bone. Here, we used an immunohistochemical approach to study whether MEPE has a role in murine long bone development and regeneration. Our data showed that MEPE protein was produced by osteoblasts and osteocytes during skeletogenesis, as early as 2 days post-natal. During non-stabilized tibial fractures healing, which heal through endochondral ossification, MEPE expression was first detected in fibroblast-like cells within the callus by 6 days post-fracture. By 10 and 14 days post-fracture (the hard callus phase of repair), MEPE was expressed within late hypertrophic chondrocytes and osteocytes in the regenerating tissues. MEPE became externalized in osteocyte lacunae during this period. By 28 days post-fracture (the remodeling phase of repair), MEPE continued to be robustly expressed in osteocytes of the regenerating bone. We compared the MEPE expression profile with that of alkaline phosphatase, a marker of bone mineralization. We found that both MEPE and alkaline phosphatase increased during the hard callus phase of repair. In the remodeling phase of repair, MEPE expression level remained high while alkaline phosphatase activity decreased. We also examined the MEPE expression during cortical bone defect healing, which heal through intramembranous ossification. MEPE immunostaining was found within fibroblast-like cells, osteoblasts, and osteocytes in the regenerating bone, through 5 days to 21 days post-surgery. Thus, MEPE appears to play a role in both long bone regeneration and later stages of skeletogenesis.

### Keywords

cartilage; osteomalacia; hypophosphatemia; osteogenesis; immunostaining

### Introduction

Matrix extracellular phosphoglycoprotein (*MEPE*, also called *OF45*) is a novel gene initially identified in oncogenic hypophosphatemic osteomalacia (OHO), a rare syndrome of rickets/osteomalacia and hypophosphatemia associated with a coexisting tumor (Argiro et al., 2001; Nelson et al., 1997; Petersen et al., 2000; Rowe et al., 2000). MEPE protein shares structural similarity with other bone and dentin mineral matrix phosphoglycoproteins (Rowe et al., 2000) and like these other molecules, is expressed within osteocytes of adult bone (Petersen et al., 2000; Rowe et al., 2000). *In vitro*, MEPE is expressed by differentiated osteoblasts and its expression is markedly increased during osteoblast-mediated matrix mineralization (Argiro et al., 2001; Petersen et al., 2000). *MEPE*<sup>-/-</sup> knockout mice have a phenotype of increased bone mass in the femur (Gowen et al., 2003). Bone marrow cultures from *MEPE*<sup>-/-</sup> mutant mice show increased osteoblast number and osteoblast activity (Gowen et al., 2003). Collectively,

\*Author to whom correspondence should be addressed: Department of Orthopaedic Surgery, University of California at San Francisco, 533 Parnassus Avenue, San Francisco, CA 94143-0514, Fax: 415 476 1128, Phone: 415 502 4945, colnot@itsa.ucsf.edu.

these studies indicate that MEPE is a bone metabolism regulator, and that its primary function might be inhibiting bone formation.

In past decades, research on bone biology has not only advanced our knowledge of fetal skeletogenesis, but it has also provided clues as to how we may augment or stimulate bone regeneration in cases of delayed skeletal repair. Bone morphogenetic proteins, transforming growth factors, and fibroblast growth factors may enhance bone formation (Lieberman et al., 2002; Sandhu and Khan, 2003; Valentin-Opran et al., 2002). Our interest in MEPE arose from its role as a bone metabolism regulator and as a potential novel target for enhancing fracture healing. As a first step towards testing this potential, we used an immunohistochemical approach to study MEPE protein expression during murine long bone skeletogenesis and during tibia fracture and cortical bone defect healing.

## Materials and methods

### Collection of embryonic and postnatal murine humeri

Raven wild-type mice were mated during a 3 hours period, which resulted in a timed pregnancy where 12pm of the second day was considered as embryonic day 1 (e1.0). Humeri of e15.0, e18.0 embryos, as well as postnatal mice of 2 days, 7 days, 16 days, and 12 weeks were collected.

### Generation of non-stabilized fractures

Raven wild-type mice were used in this study. For all surgical procedures, 6 month old, 30–35 g male mice were used. The surgical procedure followed established protocols approved by UCSF Committee on Animal Research. Mice were given an intraperitoneal injection of 2 % Avertin, 0.015 ml/g body weight, to provide approximately 15–20 min of deep anesthesia. Closed non-stabilized transverse mid-diaphyseal fractures of the tibia were created with a three-point bending apparatus as described previously (Thompson et al., 2002). Radiographs were taken immediately after fracture to confirm the extent of fracture. After recovery, animals were allowed to ambulate ad libitum and analgesics were provided for the first 48 hours (Buprenorphine, ZT Sigma, St. Louis, MO). Mice were carefully monitored at frequent intervals for any signs of infection and discomfort. Mice were sacrificed by cervical dislocation after Avertin anesthesia at 3, 6, 10, 14, and 28 days post-fracture. Fractured tibias were harvested for histological and MEPE immunohistochemical study.

### Generation of cortical bone defect

Raven wild-type mice were used as that in fracture study. Under avertin-induced deep anesthesia, an anterior longitudinal incision was made over the proximal tibia, and a 1.0 mm diameter hole was created in the diaphysis, proximal to the tibia tubercle, using a dental drill. Drilling was halted as soon as the medullary cavity was accessed, thereby leaving the far cortex intact. After recovery, animals were allowed to ambulate ad libitum. Mice were sacrificed and the tibias were harvested at 3, 6, 10, 14, and 28 days post-surgery.

### Tissue preparation

All skeletal tissues were collected and fixed at 4°C in 4% PFA overnight. Tissues were decalcified at 4°C in 19% EDTA, pH 7.4 for 2–14 days. All skeletal tissues were prepared for analyses by dehydration in a graded ethanol series and embedded in paraffin (Albrecht et al., 1997). 7 µm sections were prepared from postnatal tissues. 10 µm sections were prepared from adult skeletal tissues.

## Histological staining

For histological study, Safranin O/Fast Green staining was used to show the cartilage formation and its replacement by new bone during skeletogenesis and non-stabilized fracture healing. The cartilage appeared in red color, while the bone and soft tissue in green color.

To show the new bone formation during the cortical bone defect healing, Trichrome staining was performed on the slides adjacent to that used in MEPE immunostaining. The bone was stained blue and soft tissue red.

## Alkaline phosphatase staining

To visualize bone mineralization during non-stabilized fracture, alkaline phosphatase (AP) staining was performed on slides adjacent to those used for immunostaining. Slides were dewaxed, incubated in alkaline phosphatase buffer (100mM Tris PH9.5, 50mM MgCl<sub>2</sub>, 10mM NaCl, and 0.1% Tween20, dH<sub>2</sub>O) at 4°C for 24 hours, then in BM-purple solution (Roche Diagnostic Corporation, Indianapolis, IN) at 4°C overnight and lightly counterstained with eosin. A dark blue color reaction indicated alkaline phosphatase activity.

## MEPE immunostaining

The primary antibody (Acologix, Inc. Emeryville, CA. PAB-1274) used was a rabbit-anti-mouse polyclonal antibody generated against a peptide segment of mouse MEPE. Tissue sections were de-waxed and rehydrated from a graded ethanol series into 1× PBS (pH 7.4), quenched with 5% H<sub>2</sub>O<sub>2</sub> in PBS for 5 min, pretreated with 0.1% trypsin for 15 min (5 min for embryonic tissues) and 0.1 M glycine for 1 min, blocked by 5% powdered milk for 10 min, 0.1% ovalbumin for 10 min, and 5% goat serum for 30 min, then incubated with the primary antibody overnight, 4°C, at a dilution of 1:250 (for negative control, 5% goat serum was used instead of primary antibody in this step). Sections were then incubated with biotinylated goat anti-rabbit IgG, and streptavidin-horseradish peroxidase (Amersham RPN 1231). Immunostaining was visualized using DAB (diaminobenzidine) as a substrate. Counterstaining was performed using Fast Green or Methyl Green.

## Results

### MEPE expression during long bone development

Long bones, including the humeri and tibias, form through endochondral ossification. We first analyzed fetal skeletal elements for evidence of MEPE expression and found that although the primary ossification center formed and osteoblasts appeared by embryonic day 15, we did not detect MEPE immunoreactivity until 2 days post-natal (data not shown and Fig. 1). At 2 days post-natal, MEPE immunostaining was detectable in the osteoblasts lining the calcified cartilage cores in primary metaphyseal bone and in osteocytes embedded in cortical bone matrix (Fig. 1A–F). Although MEPE immunoreactivity was not found in the extracellular matrix surrounding osteoblasts, the protein was detected on the wall of osteocyte lacunae. Some bone marrow cells were also immunopositive for MEPE (Fig. 1A–F).

In 12 week-old mice whose skeleton is mature, MEPE was detected in osteocytes of cortical and trabecular bone as well as in bone marrow cells (Fig. 1G–I). We found that the distribution of MEPE immunoreactivity within osteocytes of adult bone was comparable to its distribution during postnatal long bone development. MEPE immunostaining was associated both with the cell body and with the wall of osteocyte lacunae, suggesting that MEPE was secreted by osteocytes (Fig. 1G–I).

### MEPE expression during non-stabilized tibia fracture healing

Non-stabilized tibia fractures heal through endochondral ossification, during which a cartilage template is formed and replaced by bone (Colnot et al., 2003; Thompson et al., 2002). By 3 days post-fracture (Fig. 2A–C), which corresponds to the inflammatory phase of fracture healing, mesenchymal cells at the site of injury began to differentiate into either chondrocytes or osteoblasts (Le et al., 2001). This time point precedes proteoglycan staining. Alkaline phosphatase staining was detected in the periosteum and endosteum (Fig. 2B), but not in the fracture site, suggesting that cells in the fracture site had not begun to deposit mineral. We did not detect MEPE immunostaining in the fracture callus by this time (Fig. 2C).

At 6 days post-fracture (Fig. 2D–F), which represents the soft callus phase of fracture healing, a large callus had formed and proteoglycan-positive cartilage was evident within the callus. The first evidence of new bone was noticed adjacent to the periosteum (Thompson et al., 2002). Comparing to 3 days post-fracture, alkaline phosphatase activity was stronger in both the periosteum and the endosteum adjacent to the fracture site and around the cartilage islands, indicating the cells had begun to deposit mineral in the callus (Fig. 2E). Weak MEPE immunostaining was detectable in fibroblast-like cells within the callus (Fig. 2F).

By 10 days post-fracture (Fig. 2G–J), which corresponds to an early time point of the hard callus phase of fracture healing, a bulk of cartilage was seen throughout the callus. Alkaline phosphatase staining was robust in the cartilage callus, suggesting that the cartilage matrix was undergoing active mineralization. The cartilage callus underwent hypertrophy and new bone began to form around the cartilage islands and in the periosteal reaction area (Colnot et al., 2003). MEPE immunostaining was detected within the late hypertrophic chondrocytes at the chondro-vascular junction (Fig. 2I). Osteocytes embedded in the newly formed bone matrix presented intracellular immunostaining. At this stage the wall of osteocytes lacunae did not exhibit detectable MEPE immunoreactivity (Fig. 2J).

By 14 days post-fracture (Fig. 2K–N), which corresponds to a later time point of the hard callus phase of fracture healing, the fracture callus was composed of hypertrophic cartilage, being actively replaced by bone. Alkaline phosphatase staining was detected throughout the callus, suggesting high activity of mineralization (Fig. 2L). MEPE immunostaining was evident in the hypertrophic chondrocytes and their surrounding extracellular matrix at the ossification front (Fig. 2M). Strong MEPE immunoreactivity was also detected within osteoblasts and osteocytes in the new bone (Fig. 2N). MEPE immunostaining was now seen in the extracellular space around osteocytes, indicating that osteocytes had started to secrete the protein.

By 28 days post-fracture (Fig. 2O–R), during the remodeling phase of fracture healing, the callus was composed primarily of bone, which was undergoing extensive remodeling. Alkaline phosphatase activity was greatly diminished, showing a decrease in osteoblast activity and mineralization (Fig. 2P). MEPE immunostaining was strong in osteocytes in the new bone and in the osteoblasts adjacent to trabecular bone (Fig. 2Q, R).

Throughout the course of fracture repair, MEPE immunostaining in the mature osteocytes of the cortical bone and in bone marrow did not show any detectable changes compared to normal adult bone (Fig. 1, and data not shown). The results indicated that the injury and the healing process did not affect the basal level of MEPE expression in normal bone.

### MEPE expression during repair of a cortical bone defect

Trichrome staining showed that a 1.0 mm cortical bone defect was filled with new bone by 10 days post-surgery. The new bone underwent remodeling and a new cortex was formed by 21 days (Fig. 3). During this process, no cartilage was detected in the defect by Safranin O/Fast Green staining (data not shown), demonstrating that this type of bone defect heals through

intramembranous ossification, whereby mesenchymal cells differentiate directly into osteoblasts.

We found that by 5 days post-surgery, MEPE immunostaining was detectable in fibroblast-like cells within the defect (Fig. 3A, B). By 10 days (Fig. 3D–F), MEPE protein was detected in osteocytes within the new bone filling the defect. By 21 days (Fig. 3G–I), strong MEPE expression was obvious in osteocytes of the newly formed cortex and in their surrounding lacunae.

## Discussion

MEPE has been recently characterized as a novel bone metabolism regulator, however its function is still poorly understood (Argiro et al., 2001; Gowen et al., 2003; Guo et al., 2002; MacDougall et al., 2002; Quarles, 2003; Rowe et al., 2000). To better understand the role of MEPE in bone formation, repair, and remodeling we carried out a detailed description of MEPE expression profile during long bone skeletogenesis, in normal adult bone, and during the process of tibia fracture and cortical defect repair.

### MEPE in post-natal skeletogenesis and in adult bone

In this study, we used an immunohistochemical approach and found that MEPE protein was expressed during post-natal skeletogenesis. MEPE protein was first detected in osteocytes of mouse humeri by 2 days post-natal. These results indicated that during bone development, MEPE might not be involved in the initiation of ossification and mineralization that take place in late embryonic stages. Instead, MEPE might play a role during the late stage of bone growth and remodeling. Previous studies report the localization of *MEPE* mRNA in the rat mandible by embryonic day 17 and sustained expression of *MEPE* at later time points (Igarashi et al., 2002). The differences between these data and ours suggest that there might be a delay between *MEPE* mRNA expression and protein expression. MEPE protein might also be present at a very low level during late embryonic stages, which was undetectable by our immunostaining protocol. Another possibility is that there is a difference between the profile of MEPE expression in long bones, which form through endochondral ossification, and the mandible, which forms through intramembranous ossification. Since the program of bone development is in large part recapitulated during bone healing, we addressed the possibility that MEPE also plays a role in bone healing. We examined cells at sites of skeletal injury, which healed through endochondral ossification (i.e., the non-stable tibia fracture), or by intramembranous ossification (i.e., a cortical defect injury).

### MEPE in bone regeneration

Our analyses revealed that MEPE protein was not detected during the early stage of non-stabilized tibia fracture repair (3 days post-fracture). Its expression in the cortex and the bone marrow adjacent to fracture site was not significantly altered by the injury. These findings suggest that MEPE might not take part in the inflammatory phase of fracture healing. During the soft callus (6–10 days post-fracture), hard callus (14 days post-fracture), and remodeling (28 days post-fracture) phases, expression of MEPE was detectable within late hypertrophic chondrocytes, osteoblasts, and osteocytes in the callus. The amount of MEPE protein increased in parallel with alkaline phosphatase activity during the hard callus phase. In addition, MEPE protein appeared to become externalized from osteocytes during this period. These results are consistent with MEPE being a mineralization regulator.

During the remodeling phase of tibia fracture healing, the amount of MEPE protein did not attenuate along with the diminished activity of alkaline phosphatase. The expression pattern of MEPE protein during the healing of a tibial cortical defect was similar to that during non-

stabilized fracture repair, with increased immunoreactivity towards the late stages of healing. These findings reinforced the role of MEPE as a negative regulator of bone mineralization (Gowen et al., 2003). MEPE might play an adjunct role in the mineralization, comparing with other major factors such as parathyroid hormone (PTH), calcitonin, and vitamin D (Boden and Kaplan, 1990; Doppelt, 1984; Tam et al., 1986; Wallach et al., 1999). This conclusion is further supported by the phenotype analysis of *MEPE* knockout mice, whose bone abnormality is relatively subtle, comparing to the severe bone diseases caused by hyperparathyroidism and deficiency of vitamin D (Doppelt, 1984; Gowen et al., 2003).

Taken together, our results show that MEPE is expressed during long bone skeletogenesis and regeneration. Further gain or loss of function experiments may elucidate the exact action of MEPE during bone mineralization. MEPE or its derivatives may turn out to be novel targets for the treatment of abnormal phosphate metabolism or bone healing.

## Acknowledgments

The authors would like to thank D. Hu for expert technical assistance and Acologix, Inc. for providing the primary MEPE antibody. This work was supported by funds from R01 DE31497 and P60 DE13058 (J.A.H.), K08 AR02164 (T.M.), and R01 AR46238 (Z. Werb).

## Reference list

- Albrecht, UEG.; Helms, JA.; Lin, H. Visualization of gene expression patterns by in situ hybridization. In: Daston, GP., editor. *Molecular and cellular methods in developmental toxicology*. Boca Raton, FL: CRC Press; 1997. p. 23-48.
- Argiro L, Desbarats M, Glorieux FH, Ecarot B. Mepe, the gene encoding a tumor-secreted protein in oncogenic hypophosphatemic osteomalacia, is expressed in bone. *Genomics* 2001;74:342–351. [PubMed: 11414762]
- Boden SD, Kaplan FS. Calcium homeostasis. *Orthop Clin North Am* 1990;21:31–42. [PubMed: 2404236]
- Colnot C, Thompson Z, Miclau T, Werb Z, Helms JA. Altered fracture repair in the absence of MMP9. *Development* 2003;130:4123–4133. [PubMed: 12874132]
- Doppelt SH. Vitamin D, rickets, and osteomalacia. *Orthop Clin North Am* 1984;15:671–686. [PubMed: 6387576]
- Gowen LC, Petersen DN, Mansolf AL, Qi H, Stock JL, Tkalcevic GT, Simmons HA, Crawford DT, Chidsey-Frink KL, Ke HZ, et al. Targeted disruption of the osteoblast/osteocyte factor 45 gene (OF45) results in increased bone formation and bone mass. *Journal of Biological Chemistry* 2003;278:1998–2007. [PubMed: 12421822]
- Guo R, Rowe PS, Liu S, Simpson LG, Xiao ZS, Darryl Quarles LD. Inhibition of MEPE cleavage by Phex. *Biochemical and Biophysical Research Communications* 2002;297:38–45. [PubMed: 12220505]
- Igarashi M, Kamiya N, Ito K, Takagi M. In situ localization and in vitro expression of osteoblast/osteocyte factor 45 mRNA during bone cell differentiation. *Histochem J* 2002;34:255–263. [PubMed: 12588003]
- Le AX, Miclau T, Hu D, Helms JA. Molecular aspects of healing in stabilized and non-stabilized fractures. *J Orthop Res* 2001;19:78–84. [PubMed: 11332624]
- Lieberman JR, Daluiski A, Einhorn TA. The role of growth factors in the repair of bone. *Biology and clinical applications*. *J Bone Joint Surg Am* 2002;84-A:1032–1044. [PubMed: 12063342]
- MacDougall M, Simmons D, Gu TT, Dong J. MEPE/OF45, a new dentin/bone matrix protein and candidate gene for dentin diseases mapping to chromosome 4q21. *Connect Tissue Res* 2002;43:320–330. [PubMed: 12489176]
- Nelson AE, Robinson BG, Mason RS. Oncogenic osteomalacia: is there a new phosphate regulating hormone? *Clin Endocrinol (Oxf)* 1997;47:635–642. [PubMed: 9497867]
- Petersen DN, Tkalcevic GT, Mansolf AL, Rivera-Gonzalez R, Brown TA. Identification of osteoblast/osteocyte factor 45 (OF45), a bone-specific cDNA encoding an RGD-containing protein that is highly

expressed in osteoblasts and osteocytes. *Journal of Biological Chemistry* 2000;275:36172–36180. [PubMed: 10967096]

Quarles LD. FGF23, PHEX, and MEPE regulation of phosphate homeostasis and skeletal mineralization. *Am J Physiol Endocrinol Metab* 2003;285:E1–E9. [PubMed: 12791601]

Rowe PS, de Zoysa PA, Dong R, Wang HR, White KE, Econs MJ, Oudet CL. MEPE, a new gene expressed in bone marrow and tumors causing osteomalacia. *Genomics* 2000;67:54–68. [PubMed: 10945470]

Sandhu HS, Khan SN. Recombinant human bone morphogenetic protein-2: use in spinal fusion applications. *J Bone Joint Surg Am* 2003;85-A(Suppl 3):89–95. [PubMed: 12925615]

Tam CS, Heersche JN, Jones G, Murray TM, Rasmussen H. The effect of vitamin D on bone in vivo. *Endocrinology* 1986;118:2217–2224. [PubMed: 3486118]

Thompson Z, Miclau T, Hu D, Helms JA. A model for intramembranous ossification during fracture healing. *J Orthop Res* 2002;20:1091–1098. [PubMed: 12382977]

Valentin-Opran A, Wozney J, Csimma C, Lilly L, Riedel GE. Clinical evaluation of recombinant human bone morphogenetic protein-2. *Clin Orthop* 2002:110–120. [PubMed: 11937870]

Wallach S, Rousseau G, Martin L, Azria M. Effects of calcitonin on animal and in vitro models of skeletal metabolism. *Bone* 1999;25:509–516. [PubMed: 10574570]

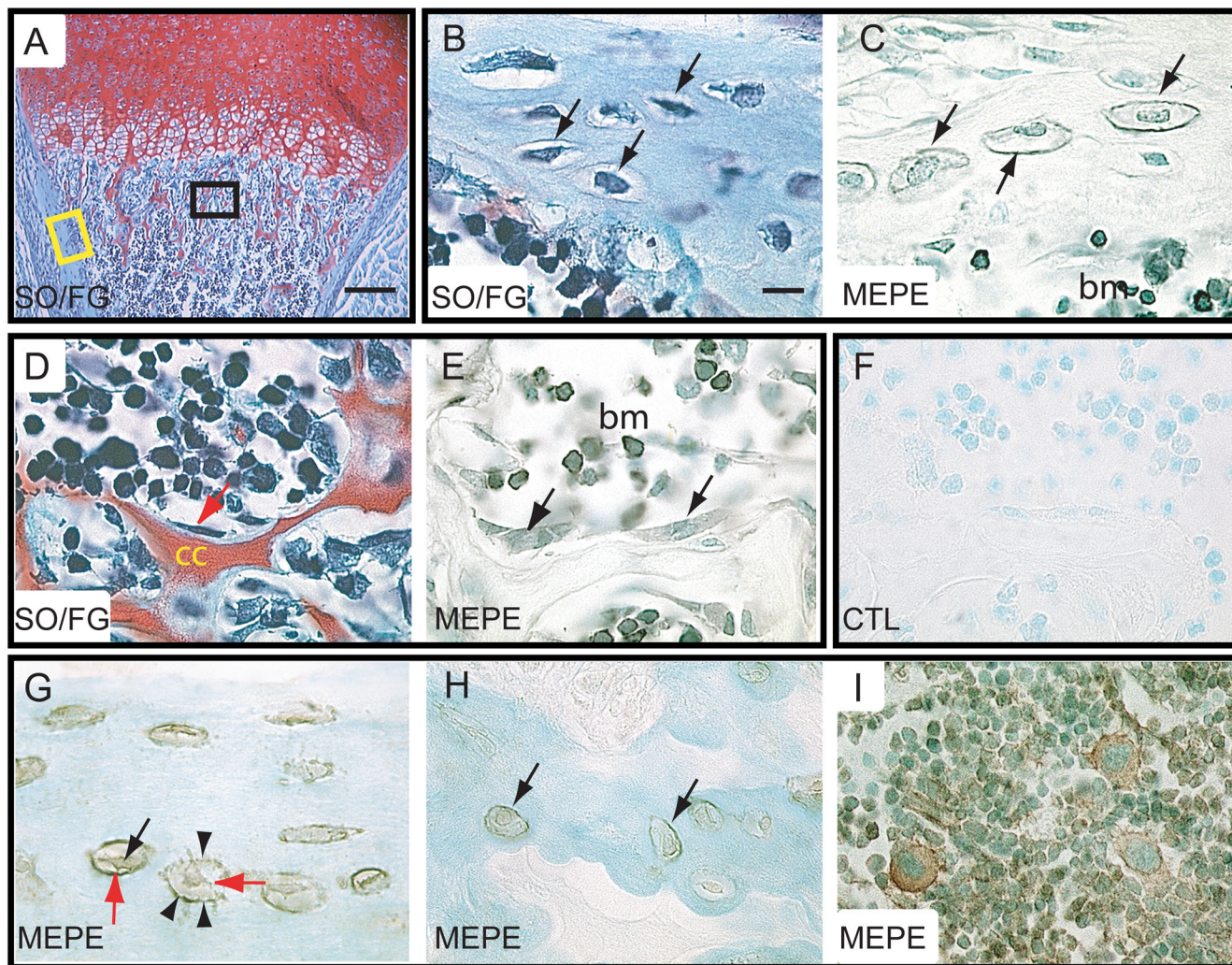


**Figure 1.** Immunolocalization of MEPE protein in developing and mature long bones. (A–F) Longitudinal sections through the humerus of a 2-day post-natal mouse. (A) SO/FG staining showed hypertrophic cartilage in the process of being replaced by trabecular bone. (B) Higher magnification of the cortex showed osteocytes (arrows) embedded in bone matrix (corresponding to yellow box in A). (C) MEPE immunostaining on an adjacent section was localized in osteocytes (arrows) of the cortex, along osteocyte lacunae (arrowheads), and in bone marrow cells. (D) Higher magnification in the metaphysis (corresponding to the black box in A) showed osteoblasts (arrow) lining the remnants of calcified cartilage (cc) matrix. (E) MEPE immunostaining on an adjacent section was detected in both osteoblasts (arrows) and bone marrow cells. (F) Negative control showed the lack of MEPE staining. (G–I) Longitudinal section through a 12-week old mouse humerus. (G) Osteocytes within cortical bone were positive for MEPE immunostaining. MEPE immunoreactivity was found intracellularly (black arrow) and on the wall of osteocyte lacunae (arrowheads). MEPE immunoreactivity was also detected in the cell processes (red arrows). (H) Osteocytes in trabecular bone were also positive for MEPE immunostaining. (I) MEPE immunostaining in bone marrow cells. bm= bone marrow, cc = calcified cartilage, SO/FG = Safranin O/Fast Green staining, CTL= control. Scale bar in A = 500  $\mu$ m, B–I = 10  $\mu$ m.



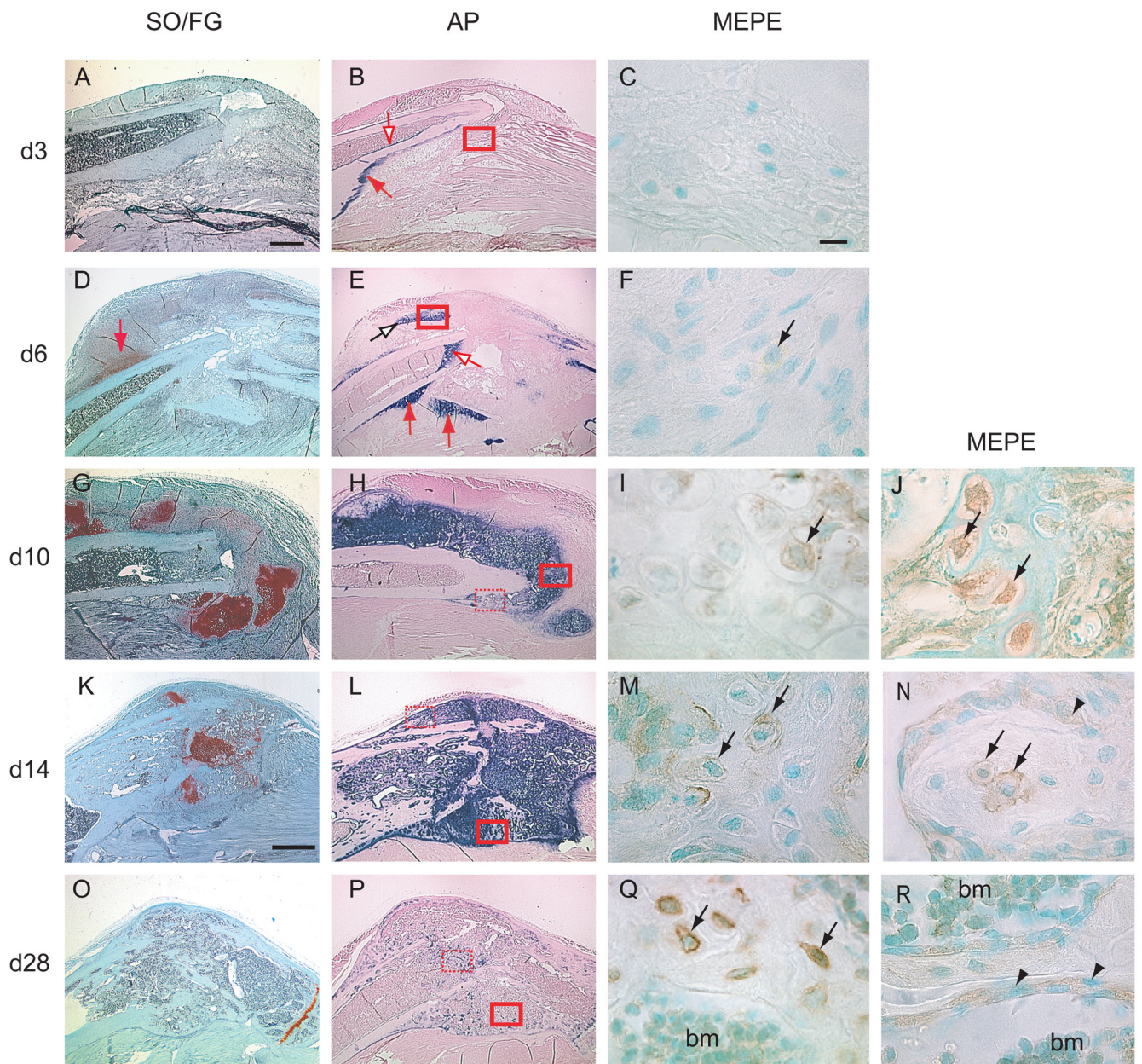


**Figure 2.** Distribution of MEPE protein in the callus tissue during non-stabilized fracture healing. (A, D, G, K, O) Safranin O/Fast Green staining on longitudinal sections through the fracture callus between 3 (d3) and 28 days (d28) post-fracture. Cartilage stained red. (B, E, H, L, P) Alkaline phosphatase (AP) staining (blue staining) on adjacent sections. (C, F, I, M, Q) MEPE immunostaining in area corresponding to solid red boxes in (B, E, H, L, P) respectively. (J, N, R) MEPE immunostaining in area corresponding to the dashed red boxes in (H, L, P) respectively. (A) At 3 days post-fracture, SO/FG staining indicated no proteoglycan accumulation, as shown by the lack of red staining. (B) Minimal AP activity was evident on the endosteum (empty arrow) and periosteum (red arrow). (C) No MEPE immunostaining was detectable around the fracture site. (D) By 6 days, cartilage islands within the callus were visible

by SO/FG staining (red arrow). (E) AP activity was seen around these cartilage islands (empty black arrow), in the periosteum (red arrows), and in the endosteum (empty red arrow). (F) Weak MEPE immunostaining was found in some of the cells within these cartilage islands (arrow). (G) By 10 days, abundant cartilage was present in the fracture callus. (H) AP activity was strong throughout the cartilage callus and in the new periosteal bone. (I) MEPE immunostaining was detectable in late hypertrophic chondrocytes within the callus (arrow). (J) MEPE immunostaining was detected in osteocytes (arrows) embedded in the new bone. MEPE immunostaining was associated with the cell body and the cell processes. (K) By 14 days, the amount of cartilage within the callus was diminished. (L) AP activity was evident throughout the callus. (M) MEPE immunostaining was found in the pericellular matrix of late hypertrophic chondrocytes (arrows) at the ossification front. (N) MEPE immunostaining was localized in the osteocytes and in the lacunae (arrows) within the newly formed trabecular bone. Osteoblasts (arrowheads) lining the trabecular bone exhibited weak MEPE immunostaining. (O) By 28 days, the hypertrophic cartilage was completely resorbed and (P) AP activity was decreased. (Q) Strong MEPE immunostaining was seen in osteocytes in the new bone (arrows). (R) Osteoblasts (arrowheads) adjacent to trabecular bone and bone marrow cells (bm) were also positive for MEPE immunostaining. bm = bone marrow. Scale bars: A, B, D, E, G, H = 0.5mm. K, L, O, P = 1mm. MEPE = 10  $\mu$ m.

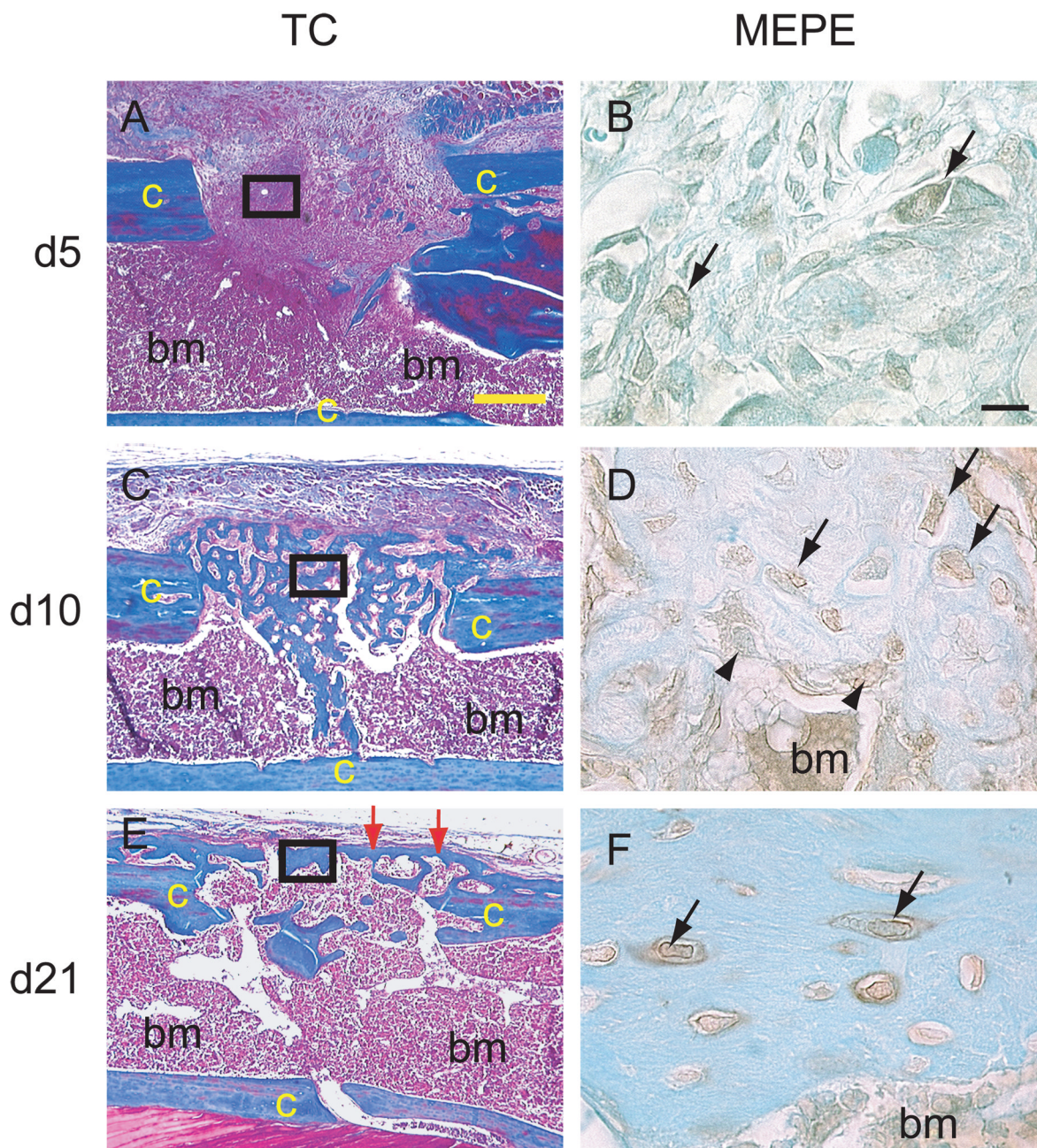


**Figure 3.**

Immunodetection of MEPE protein during healing of a cortical bone defect. (A, C, E) Longitudinal sections through a 1mm cortical bone defect stained with Trichrome. (B, D, F) MEPE immunostaining on adjacent sections corresponding to the area of solid black boxes in (A,C, E) respectively. (A) By 5 days post-surgery, granulation tissue filled the defect. (B) Weak MEPE immunostaining was detected in fibroblastic cells within the defects (arrows). (C) By 10 days, new bone had formed in the cortical defect. (D) Osteocytes (arrows) and osteoblasts (arrowheads) in the new bone exhibited MEPE immunostaining. (E) By 21 days, new bone within the cortical defect was remodeled and a new cortex had formed (arrows). (F) MEPE immunostaining was strong in the osteocytes and their pericellular matrix within the new cortex

(arrows). Bone marrow cells were also positive for MEPE immunostaining. c = cortex, bm = bone marrow, TC = Trichrome staining. Scale bars: A, C, E = 300  $\mu\text{m}$ , B, D, F = 10  $\mu\text{m}$ .